Projections of Climate Change over Non-boreal East Europe During First Half of Twenty-First Century According to Results of a Transient RCM Experiment

Shimon O. Krichak, Pinhas Alpert, and Pavel Kunin

Department of Geophysics and Planetary Sciences, Raymond and Beverly Sackler Faculty of Exact Sciences, Tel Aviv University, Ramat Aviv, 69978, Tel Aviv, Israel, E-mail: shimon@cyclone.tau.ac.il

Abstract. Climate change trends over the southern east-Europe are evaluated according to results of a climate simulation experiment with the ICTP RegCM3 regional climate model driven from the lateral boundaries by results of ECHAM5/MPI-OM1 transient climate simulation from 1960 to 2060 (SRES A1B emission scenario after 2001). The trends projected include – precipitation: winter and spring – rise over the central east-Europe and drop over the eastern Mediterranean region, summer-autumn – drop over east-Europe and northern eastern-Mediterranean, rise over the Middle East (especially in autumn); 2-m air temperature: winter and spring – rise over the whole region with a maximum over its eastern and north-eastern (especially) and south-eastern parts, summer – rise with a maximum over the Middle East and minimum over north-eastern part, autumn – rise with maximum over the Caspian, Black Seas and northern areas of the European Territory of Russia.

Keywords: regional climate model, climatic change, East Europe

Introduction

Anthropogenic emission of greenhouse gases (GHG) has been recognized as the main factor of the global climate change of the post-industrial era (IPCC 2007). Results of a high-resolution regional climate change simulation experiment over southeastern Europe for the period 1960–2060 are discussed below. Description of the experiment's setup is given in the section "Experimental Setup and Data Used". Obtained in the experiment were projections of the climate change process over the region from recent past to near future which are discussed in the section "Results". Discussion and conclusion are given in the last section.

P.Y. Groisman and S.V. Ivanov (eds.), *Regional Aspects of Climate-Terrestrial-Hydrologic Interactions in Non-boreal Eastern Europe*,

© Springer Science + Business Media B.V. 2009

Experiment Setup and Data Used

Regional climate model (Caya and Biner 2004; Christensen and Christensen 2004; Giorgi et al. 2004; Krichak et al. 2007; Semmler and Jacob 2004) simulation of climate of the southern Europe region has been performed. The model adopted is the state of science, third generation RegCM3 (Pal et al. 2007) of the International Center for Theoretical Physics (ICTP). The following parameters characterize the model configuration: 50 km horizontal resolution, 14 vertical sigma levels, the model top is located at 80 hPa, five levels located below ~1,500 m represent the planetary boundary layer. The model domain covers an area including a large part of Europe, eastern north-Africa and the Middle East (Fig. 6.1). The lateral boundary relaxation zone covers 11 grid intervals. A smoothing of terrain inside of the relaxation zone is performed. The physical parameterizations chosen [radiation (Kiel et al. 1996); land-surface model (Dickinson et al. 1993; Gao et al. 2006); planetary boundary layer (Holtslag et al. 1990); cumulus parameterization (Grell 1993; Fritsch and Chapell 1980); ocean flux parameterization (Zeng et al. 1998), lateral boundary treatment (Davies and Turner 1977) – for references and further details see Pal et al. (2007) are selected according to results of earlier evaluations (Krichak et al. 2007).

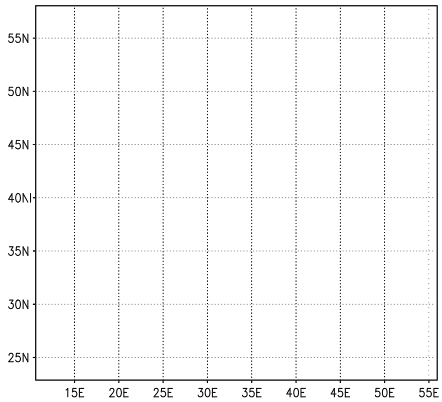

Fig. 6.1. Model simulation domain.

The driving data used are from an atmosphere–ocean general circulation model (AOGCM) experiment with fifth-generation ECHAM5/ MPI-OM model of the Max-Plank Institute for Meteorology, Hamburg (Roeckner et al. 2003). The atmospheric model was run with T63 truncation (1.875° x 1.875° spatial resolution) and 31 hybrid vertical levels (Roeckner et al. 2003). The ocean model uses a conformal mapping grid with a horizontal grid spacing of 1.5° and 40° vertical levels. For the future climate projection (IPCC 2007) the greenhouse gases (GHG) emission scenario A1B (SRES A1B, hereafter A1B) was employed (after 2001) both in the AOGCM and RCM simulations. Results produced in the experiment are presented below in the patterns with differences between multi-year mean precipitation (*Prec*) and 2 m air temperature (*T2m*) determined for the two 30-year time-periods [current (1961–1990, CT) and near-future (2021–2050)]. Area of the analysis is limited by 30° N–57° N; 15° E–50° E.

Results

Simulation of current climate

Results of simulation of *Prec* and *T2m* for warm AMJJASO and cold NDJFM seasons under the current climate (1961–1990) conditions (not presented) have been compared to the data from observation-based archive of the Climate Research Unit of the University of East Anglia, UK (Mitchell et al. 2004). The regional climate model (RCM) reasonably well reproduces precipitation over the Mediterranean region, where differences between simulated and observed precipitation are less than 10 mm season^{-1} . However, RCM results over and northward of the Caucasus area were less successful. A notable overestimation of the precipitation amount (especially during AMJJASO season, i.e. rains of convective origin) has been noted. Annual cycle of precipitation is well reproduced over the whole model domain however (Krichak 2008). The *T2m* patterns both for the warm and cold seasons were also reasonably well simulated – the differences between simulated and observed CT *T2m* are less ~2°C.

Simulation of anthropogenic climate change trend

The simulated in the climate change experiment trends associated with precipitation (in mm) from 1961–1990 to 2021–2050 are in given in Fig. 6.2a–d for winter (DJF), spring (MAM), summer (JJA), autumn (SON) seasons, respectively. During DJF, a negative precipitation trend (down to −60 mm) characterizes the eastern Mediterranean region (Fig. 6.2a). A precipitation rise (20–40 mm) is projected for the northern part of the area of the experiment. An area with the maximum in the positive precipitation trend (60 mm) over the south-eastern part of the Black Sea area may be noted. During spring (MAM) a zone with a precipitation drop (down to 20 mm) is found over the northeastern Mediterranean area (Fig. 6.2b). A significant rise of precipitation is projected for the northern (40 mm) and especially north-eastern (up to 60–80 mm) parts of the non-boreal east Europe.

No changes in precipitation intensity are projected over the major part of the Mediterranean region for the JJA season (Fig. 6.2c). A 20–80 mm reduction of precipitation is projected over the non-boreal east Europe and south-Caucasus areas, although a ~20–40 mm increase in precipitation is projected for the Black Sea area (Fig. 6.2c). A significant rise in the autumn (SON) precipitation is projected for the eastern Mediterranean (up to 60 mm) and Black Sea (40 mm) regions (Fig. 6.2d). A minor precipitation drop is projected for the non-boreal part of the ETR.

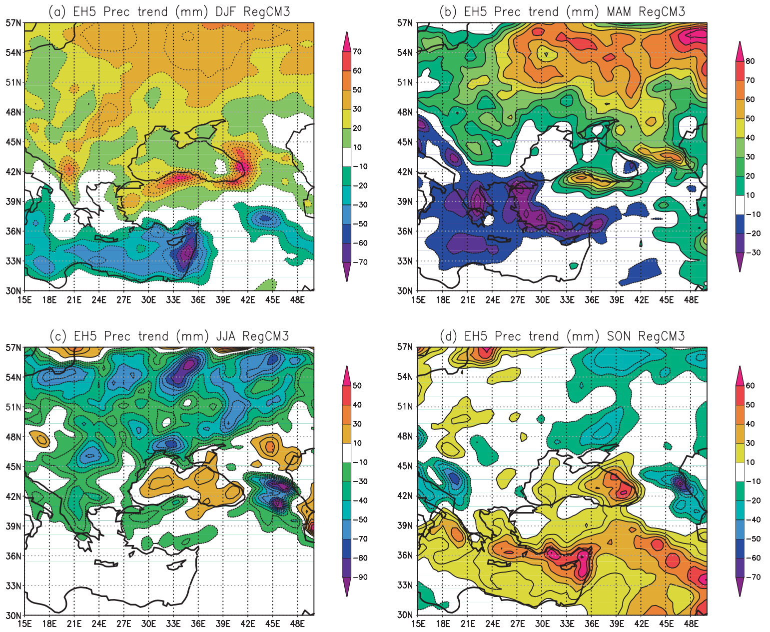

Fig. 6.2. Simulated trend of mean seasonal precipitation (**a**) winter, (**b**) spring, (**c**) summer and (**d**) autumn seasons.

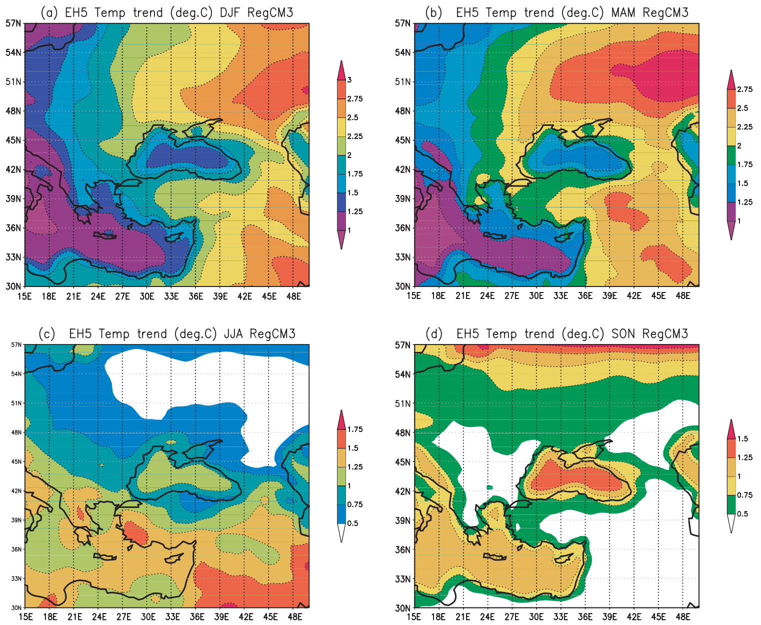

Fig. 6.3. Simulated trend of mean seasonal 2 m air temperature (**a**) winter, (**b**) spring, (**c**) summer and (**d**) autumn seasons.

Projected changes in the seasonal 2 m air temperature *(T2m)* are given in Fig. 6.3a–d. A *T2m* rise (Fig. 6.3a) is simulated over the whole area of the domain for DJF. The magnitudes of the simulated temperature rise are higher (up to ~2.5°C) over the eastern part of the pattern with one center located in the vicinity of the Persian Gulf and the second to the north of Caspian Sea area. A similar pattern of the *T2m* trend over Europe characterizes the MAM season (Fig. 6.3b). The zone with the maximum *T2m* rise (2.0–2.5°C) is found here over the non-boreal Europe northward of the Caspian Sea. Another zone with significant, although lower *T2m* rise (~2.5°C), is found over the Middle East area. A notable *T2m* rise characterizes the pattern produced in the experiment for the summer (JJA) season (Fig. 6.3c). The *T2m* trend is stronger (up to 1.5ºC) over the Middle East but is also notable over the Mediterranean Sea area. Over the east Europe the *T2m* rise is less significant (0.2–0.6°C). The pattern produced in the experiment for autumn (Fig. 6.3d, SON) is characterized by the *T2m* rise over the Mediterranean and Black Seas (~+1.0°C) over the Black Sea), and non-boreal Europe (0.5–1.0°C).

Discussion and Conclusion

A number of factors may be limiting reliability of the results presented. The accuracy of the climate simulation could be affected by the description of sub-grid processes in the relatively coarse-resolution (50 km) RCM run. Also, the physical parameterizations adopted seem to be more appropriate for the simulations of the Mediterranean climate than the more northern part of the area. A new set of the climate change simulation experiments with an optimized set of the RegCM3 physics is currently in process of realization. Reliability of the RCM results could also be affected by that of the AOGCM (i.e. driving) data as well as by that of the GHG emission scenario adopted.

Nevertheless, results of the transient RCM simulation performed for the near-future south-east Europe climate change seem to be providing useful information on the possible climate change perspectives over Europe. The climate conditions simulated for the near-future (2021–2050) differ significantly from those of the twentieth century (1961–1990) over most parts of the area of the analysis. The deduced climate change trends may be summarized as follows. Precipitation: a significant rise in DJF and MAM precipitation is projected for the central and, especially, southern east Europe. A drop in precipitation is projected for the eastern Mediterranean region however. Opposite precipitation trends are projected for the JJA and SON seasons, however, with a precipitation rise over the Middle East (especially during SON) and precipitation drop over central part of the south east Europe.

In may be summarized that the climate change experiment projects drop in the annual precipitation over the eastern and south-eastern Mediterranean region (5–20%) and rise in the parameter over the Middle East (5–20%), Black Sea area (5–

15%) and non-boreal Europe (5–10%). During DJF and MAM seasons the trends projected are characterized by a *T2m* rise over eastern part of the non-boreal Europe. The temperature trend seems to be associated with weakening of the Siberian High system. The area with the maximum *T2m* rise in the JJA pattern (Fig. 6.3c) is found over southeastern part of the domain – indicating the role of the sea surface temperature rise in the Arabian Sea in the projected climate change process over southeastern Europe. A *T2m* rise is projected also over the areas located close to Mediterranean Sea, Black Sea, and Caspian Sea which seem to be playing an important role in the climate change process over east Europe.

Acknowledgments. The research was supported by German-Israeli research grant (GLOWA – Jordan River) from the Israeli Ministry of Science and Technology; and the German Bundesministerium fuer Bildung und Forschung (BMBF); research grant no. 0603414981 from the Water Authority of Israel (Modeling Climate in Israel of the Recent Past and Future) and integrated project granted by the European Commission's Sixth Framework Programme, Priority 1.1.6.3 Global Change and Ecosystems (CIRCE), Contract no.: 036961. We are grateful to Dr. Filippo Giorgi and his colleagues at the Physics of Weather and Climate (PWC) Section of the Abdus Salam International Centre for Theoretical Physics (ICTP), Trieste for providing expertise on using RegCM3. The driving data from the ECHAM5 climate change simulation experiment have been obtained from the Max-Plank Institute for Meteorology, Hamburg. Special thanks also go to B.Sc. students Naama Reicher and Netta Tsur for their help in analysis of the RCM results.

References

Caya D, Biner S (2004) Internal variability of RCM simulations over an annual cycle. Climate Dynamics, 22: 33–46.

Christensen JH, Christensen OB (2003) Climate modelling: severe summertime flooding in Europe. Nature 421: 805–806.

Davies HC, Turner RE (1977) Updating prediction models by dynamical relaxation: An examination of the technique, Quart. J. Roy. Meteorol. Soc., 103: 225–245.

Dickinson RE, Henderson-Sellers A, Kennedy PJ (1993) Biosphere-Atmosphere Transfer Scheme (BATS) version 1E as coupled to the NCAR Community Climate Model, Tech. Rep. TN-387+STR, NCAR, Boulder, Colorado, 72 p.

Fritsch JM, Chapell CF (1980) Numerical prediction of convectively driven mesoscale pressure systems. Part I: Convective parameterization. J. Atmosph. Sci. 37: 1722–1733.

Gao X, Pal JS, Giorgi F (2006) Projected changes in mean and extreme precipitation over the Mediterranean region from a high resolution double nested RCM simulation, Geophys. Res. Lett, 33, L03706, doi:10.1029/2005GL024954.

Giorgi F, Bi X, Pal JS (2004) Mean, interannual variability and trends in a regional climate change experiment over Europe. II. Climate change scenarios (2071–2100), Climate Dynamics, 23: 839–858.

Grell GA (1993) Prognostic evaluation of assumptions used by cumulus parameterizations, Mon. Wea. Rev, 121: 764–787.

Holtslag AAM, de Bruijn EIF, Pan HL (1990) A high resolution air mass transformation model for short-range weather forecasting, Mon Wea Rev, 118: 1561–1575.

IPCC (2007) Climate change - the physical science basis. Contribution of working group I to the Fourth Assessment Report of the Intergovernmental Panel on Climate Change [Solomon, S., D. Qin, M. Manning, Z. Chen, M. Marquis, K.B. Averyt, M. Tignor and H.L. Miller (eds.)]. Cambridge University Press, Cambridge, UK/New York, USA, 996 pp.

Kiehl JT, Hack JJ, Bonan GB, Boville BA, Briegleb BP, Williamson DL, Rasch PJ (1996) Description of the NCAR Community Climate Model (CCM3), Tech. Rep. TN-420+STR, NCAR, Boulder, Colorado, 152 p.

Krichak SO (2008) Regional climate model simulation of present-day regional climate over European part of Russia with RegCM3. Russian Meteorology and Hydrology, 1: 31–41. (http://springerlink.com/content/120692/?p=b1704f828c724ceebc32cbb88bc4cd15&pi=0)

Krichak SO, Alpert P, Bassat K, Kunin P (2007) The surface climatology of the eastern Mediterranean region obtained in a three-member ensemble climate change simulation experiment. Advances in Geosciences, 12: 67–80. (www.adv-geosci.net/12/67/2007)

Mitchell TD, Co-authors (2004) A comprehensive set of high-resolution grids of monthly climate for Europe and the globe: the observed record (1901–2000) and 16 scenarios (2001–2100), Tyndall Centre Working Paper No. 55., Tyndall Centre for Climate Change Research, University of East Anglia, Norwich, UK.

Pal JS, Giorgi F, Bi X, Co-authors (2007) Regional climate modeling for the developing world: the ICTP RegCM3 and RegCNET. Bulletin of the American Meteorological Society, 88: 1395–1409.

Roeckner E, Co-authors (2003) The atmospheric general circulation model ECHAM5, Part I, Max-Plank Inst for Meteorology, Report no. 349, 127 p.

Semmler T, Jacob D (2004) Modeling extreme precipitation events – a climate change simulation for Europe. Global and Planetary Change, 44: 119–127.

Zeng X, Zhao M, Dickinson RE (1998) Intercomparison of bulk aerodynamic algorithms for the computation of sea surface fluxes using TOGA COARE and TAO data. J. Climate, 11: 2628–2644.

An Assessment of the Recent Past and Future Climate Change, Glacier Retreat, and Runoff in the Caucasus Region Using Dynamical and Statistical Downscaling and HBV-ETH Hydrological Model

Maria Shahgedanova

Department of Geography, The University of Reading, Whiteknights, PO Box 227, Reading RG6 6AB, UK, E-mail: m.shahgedanova@reading.ac.uk

Wilfried Hagg and Martina Zacios

Department of Geography, University of Munich, Munich, Germany

Victor Popovnin

Faculty of Geography, Moscow State University, Leninskie Gory, Moscow, Russia

Abstract. The paper discusses the observed and projected warming in the Caucasus region and its implications for glacier melt and runoff. A strong positive trend in summer air temperatures of 0.05°C a^{-1} is observed in the high-altitude areas providing for a strong glacier melt and continuous decline in glacier mass balance. A warming of 4–7°C and 3–5°C is projected for the summer months in 2071–2100 under the A2 and B2 emission scenarios respectively, suggesting that enhanced glacier melt can be expected. The expected changes in winter precipitation will not compensate for the summer melt and glacier retreat is likely to continue. However, a projected small increase in both winter and summer precipitation combined with the enhanced glacier melt will result in increased summer runoff in the currently glaciated region of the Caucasus (independent of whether the region is glaciated at the end of the twenty-first century) by more than 50% compared with the baseline period.

Keywords: glaciers, climate change, climate modeling, water resources, Caucasus

Introduction

The Caucasus region is a mountainous country stretching for 1,300 km from the Black Sea in the west and the Caspian Sea in the east (Fig. 7.1). Elevations in its highest part, the Greater Caucasus, spanning the border between Russia and

P.Y. Groisman and S.V. Ivanov (eds.), *Regional Aspects of Climate-Terrestrial-Hydrologic Interactions in Non-boreal Eastern Europe*,

© Springer Science + Business Media B.V. 2009